



Molecular structure and mesomorphism: Effect of tail/lateral group

Vinay S. Sharma & R. B. Patel

To cite this article: Vinay S. Sharma & R. B. Patel (2016) Molecular structure and mesomorphism: Effect of tail/lateral group, *Molecular Crystals and Liquid Crystals*, 630:1, 58-68, DOI: [10.1080/15421406.2016.1146866](https://doi.org/10.1080/15421406.2016.1146866)

To link to this article: <http://dx.doi.org/10.1080/15421406.2016.1146866>



Published online: 01 Jul 2016.



Submit your article to this journal [↗](#)



Article views: 34



View related articles [↗](#)



View Crossmark data [↗](#)

Molecular structure and mesomorphism: Effect of tail/lateral group

Vinay S. Sharma and R. B. Patel

Chemistry Department, K. K. Shah Jarodwala Maninagar Science College, Gujarat University, Ahmedabad, Gujarat, India

ABSTRACT

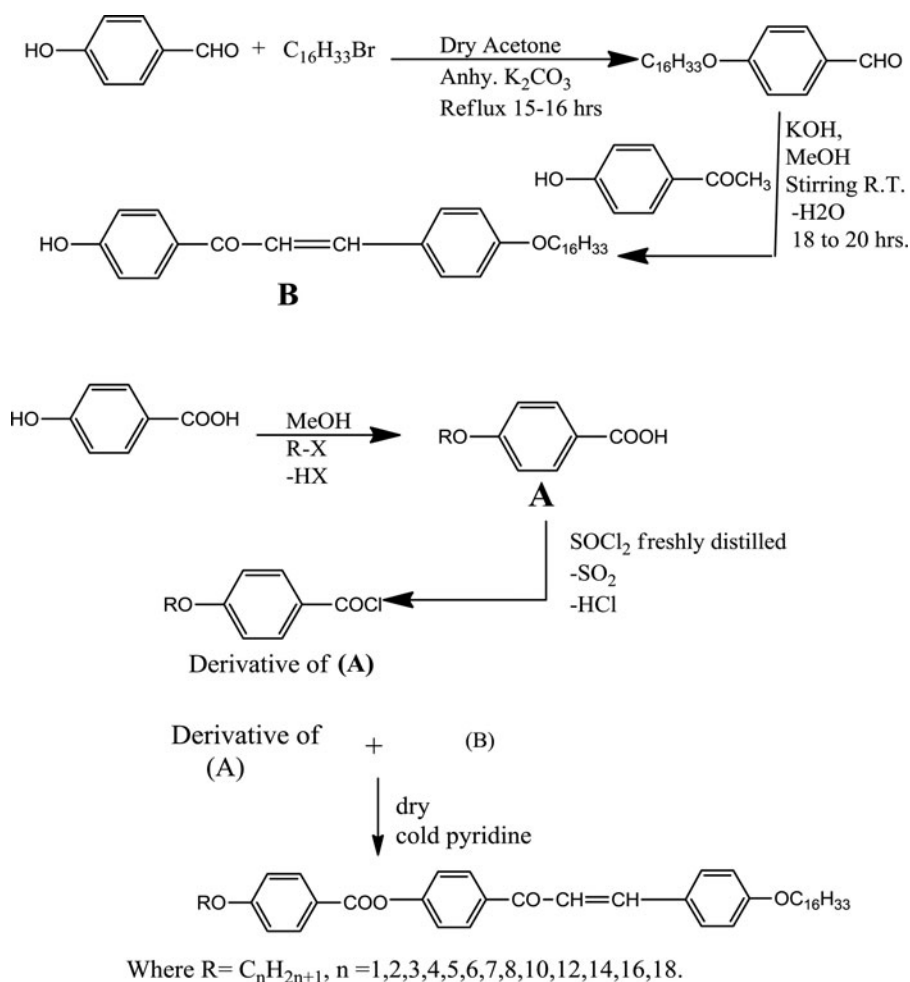
Chalconyl homologous series of novel mesogenic substances of molecular structure $\text{RO-C}_6\text{H}_4\text{-COO-C}_6\text{H}_4\text{-CO-CH:CH-C}_6\text{H}_4\text{-OC}_{16}\text{H}_{33}$ (P) has been studied with a view to understanding and establishing the effects of molecular structure on liquid crystal (LC) properties. A novel homologous series consists of 13 (C_1 to C_{18}) members. C_1 to C_5 and C_7 members are non-mesogenic and the even numbered C_6 to C_{18} homologues are enantiotropically nematogenic with absence of smectogenic property. Thermotropic properties such as phase transition temperatures and textures (threaded or Schlieren) were determined by an optical polarizing microscopy equipped with a heating stage. Analytical and spectral data confirm the molecular structure. Transition curves (Cr-N and N-I) showing phase behaviors in phase diagrams behave in a normal manner except C_{16} and C_{18} homologues, which partially deviate from normal behavior in N-I transition curve. Thermal stability for nematic on average is 113.14°C and the total mesophase length ranges from 10 to 26°C . The usual odd-even effect is absent for the N-I transition curve. The LC properties of the present novel series are compared with structurally similar known series. The present novel series is predominantly nematogenic without exhibition of smectogenic character, and is of a lower middle-ordered melting-type.

KEYWORDS

Mesomorphic; mesogen; nematic; odd-even effect; smectic

Introduction

Liquid crystalline (LC) [1] chalconyl ester derivatives play a dual role: (i) useful in LC devices within definite range of temperature, and (ii) useful in pharmaceutical preparation and therapeutic treatment to cure diseases within definite range of concentration in solution state [2–10]. The present investigation is planned with a view to understand and establish the effects of molecular structure on LC properties of thermotropic liquid crystals through the synthesis of a homologous series [11–13]. The proposed homologous series comprises three phenyl rings bonded through -COO- and -CO-CH=CH- central groups as well as varying left n-alkoxy terminal end group and a fixed $\text{-OC}_{16}\text{H}_{33}$ tail group. Many homologous series or LC materials have been reported to date [14–18], but the present chalconyl ester derivatives have a dual ability to act as thermotropic LCs and lyotropic LCs. Therefore, the novel compounds may be useful to researchers of biological sciences and technological researchers. Our investigations will be limited to (i) synthesis, (ii) characterization by analytical, thermal, and spectral



Scheme 1. Synthetic route of series-1.

data, and (iii) evaluation and interpretation of the results on the basis of molecular rigidity and flexibility [19–24] in comparison with structurally similar homologous series.

Experimental

Synthesis

4-Hydroxy benzoic acid was alkylated using suitable alkylating agents (R-X) to convert it into 4-n-alkoxy benzoic acids (A) by modified method of Dave and Vora [25]. α -4-Hydroxy benzoyl β -4'-hexadecyloxy phenyl ethylene (B) was prepared by the usual established method [26]. The acid chloride component of each 4-n-alkoxy benzoic acids was condensed with 4-hydroxy derivative of chalcone in dry cold pyridine by the usual established method [27] carefully. The chalconyl ester homologue derivatives were finally decomposed, filtered, washed, dried, and purified until constant transition temperatures were obtained using an optical polarizing microscope equipped with a heating stage. 4-Hydroxy benzoic acid, alkyl halides, thionyl chloride, MeOH, EtOH, KOH, acetone, pyridine, 4-hydroxy acetophenone, 4-hydroxy

Table 1. Elemental analysis of methoxy, pentyloxy, decyloxy, and octadecyloxy derivatives.

Sr. No.	Molecular formula	Elements found (%)		Elements theoretical (%)	
		C	H	C	H
1.	C ₃₉ H ₅₀ O ₅	78.26	8.36	77.20	8.24
2.	C ₄₃ H ₅₈ O ₅	78.89	8.86	78.05	8.80
3.	C ₄₈ H ₆₈ O ₅	79.55	9.39	78.98	9.30
4.	C ₅₆ H ₈₄ O ₅	80.38	10.04	80.05	10.01

benzaldehyde, and hexadecyl halide required for synthesis were used as received except solvents, which were dried and distilled prior to use. The synthetic route to the series is mentioned below as [Scheme 1](#).

Characterization

Representative homologues of a series were characterized by elemental analysis, mass spectrography, Infrared (IR) spectroscopy, and ¹H NMR spectra. IR spectra were recorded by Perkin–Elmer spectrum GX, ¹H NMR spectra were recorded on a Bruker using CDCl₃ as solvent. Microanalysis was performed on Perkin–Elmer PE 2400 CHN analyzer ([Table 1](#)). Transition temperature and LC properties (textures) were determined using an optical polarizing microscopy equipped with a heating stage. Texture image of some homologues for nematic phase were determined by the miscibility method ([Table 2](#)). Thermodynamic quantities enthalpy (ΔH) and entropy (ΔS = ΔH/T) are discussed qualitatively.

Analytical data

Mass spectra Homologue: ethoxy– theoretical: 612

Experimental: 612.6

IR spectra for decyloxy, hexadecyloxy, and octadecyloxy derivatives (in cm^{−1}).

Decyloxy: 717 Polymethylene (−CH₂−)_n of −OC₁₀H₂₁, 648 polymethylene (−CH₂−)_n of C₁₀H₂₁ 840 (−C−H− def. m di-substituted-para), 941 (−C−H− def. hydrocarbon), 1018 (−C−O−) str, 1373, 1303, 1249, and 1165 (−C−O str in −(CH₂)_n chain, 1465 and 1427 (−C−H− def. in CH₂), 1512 (−C=C−)str, 1604 and 1681 (−C=O group), 1735 (−COO− ester group), 2854 and 2916 (−C−H str in CH₃).

Hexadecyloxy: 648 Polymethylene (−CH₂−)_n of −OC₆H₁₃, 840(−C−H− def. m di-substituted-para), 771 polymethylene (−CH₂−) of −OC₆H₁₃, 941 (−C−H− def. hydrocarbon), 1026 and 1064 (−C−O−) Str, 1165 and 1257 (−C−O str in −(CH₂)_n chain, 1427 and 1427 (−C−H− def. in CH₂) 1504 (−C=C−) str, 1604 and 1681 (−C=O group) and (−COO− ester group), 2854 and 2924 (−C−H str in CH₃).

Octadecyloxy: 740 Polymethylene (−CH₂−)_n of −OC₁₈H₃₇, 648 polymethylene (−CH₂−)_n of C₁₈H₃₇ 817 (−C−H− def. m di-substituted para), 972 (−C−H− def. hydrocarbon), 1064 (−C−O−)

Table 2. Textures of nematic phase by miscibility method for C₆, C₁₀, C₁₄, and C₁₆.

Sr. No.	Homologue	Texture
1.	C ₆	Threaded
2.	C ₁₀	Threaded
3.	C ₁₄	Schlieren
4.	C ₁₆	Schlieren

str, 1365 and 1249, 1165 (-C-O str in $-(\text{CH}_2)_n$ chain, 1365 and 1427 (-C-H- def. in CH_2), 1504 (-C=C-) str, 1604 and 1681 (-C=O group), 1735 (-COO- ester group), 2854 and 2924 (-C-H str in CH_3).

^1H NMR spectra in CDCl_3 for heptyloxy, tetradecyloxy, and hexadecyloxy derivatives (in δ ppm).

Heptyloxy: 0.88 (t, $-\text{CH}_3$ of $-\text{C}_7\text{H}_{15}$), 1.25–1.20 (m, n-poly methylene groups of $-\text{OC}_7\text{H}_{15}$), 1.50 (m, n-poly methylene groups of $-\text{OC}_{16}\text{H}_{33}$), 3.4–3.8 (s, $-\text{OCH}_2-\text{CH}_2-$ of $\text{OC}_{16}\text{H}_{33}$), 4.0–4.2 (s, $-\text{OCH}_2-\text{CH}_2-$ of OC_7H_{15}), 7.2–7.3 (s, $-\text{CO}-\text{CH}=\text{CH}$), 8.8–8.9 (s, p-di-substituted phenyl ring).

Tetradecyloxy: 0.87 (t, $-\text{CH}_3$ of $-\text{C}_{16}\text{H}_{33}$), 0.98 (t, $-\text{CH}_3$ of $-\text{OC}_{14}\text{H}_{29}$), 1.2–1.4 (m, n-polymethylene groups of $-\text{OC}_{16}\text{H}_{33}$), 1.5–1.8 (m, n-polymethylene groups of $-\text{OC}_{14}\text{H}_{29}$), 2.6 (s, $-\text{OCH}_2$), 3.4 (s, $-\text{OCH}_2-\text{CH}_2-$ of $\text{OC}_{14}\text{H}_{29}$), 4.0–4.2 (s, $-\text{OCH}_2-\text{CH}_2-$ of $\text{OC}_{16}\text{H}_{33}$), 6.9–7.2 (s, $-\text{CO}-\text{CH}=\text{CH}$), 7.5–7.7 (s, p-substituted phenyl ring).

Hexadecyloxy: 0.86 (t, $-\text{CH}_3$ of $-\text{C}_{16}\text{H}_{33}$), 0.89 (t, $-\text{CH}_3$ of $-\text{OC}_{16}\text{H}_{33}$) 1.2 to 1.4 (m, n-polymethylene group of $-\text{OC}_{16}\text{H}_{33}$), 3.4 (s, $-\text{OCH}_2-\text{CH}_2$ of $-\text{OC}_{16}\text{H}_{33}$), 3.4 (s, $-\text{OCH}_2-\text{CH}_2$ of $-\text{OC}_{16}\text{H}_{33}$), 4.0–4.2 (s, $-\text{OCH}_2-\text{CH}_2$ of $-\text{OC}_{16}\text{H}_{33}$), 6.7–7.3 (s, $-\text{CO}-\text{CH}=\text{CH}$), 7.4 to 7.7 (s, p-substituted phenyl ring).

Results and discussion

Phase transition temperatures of novel chalconyl ester homologous series are lowered on linking 4-n-alkoxy benzoic acids with α -4-hydroxy benzoyl β -4'-hexadecyloxy ethylenes (m.p. 102.0°C , yield 67%) in dry cold pyridine. Mesomorphism commences from the hexyloxy (C_6) homologue in even numbered members as mentioned in Table 3 of a series. None of the odd numbered homologues from C_1 to C_7 exhibit mesomorphism. Only nematogenic mesomorphism is exhibited by C_6 to C_{18} except C_7 homologue, i.e. C_1 to C_5 and C_7 members are non-mesogenic. Smectogenic character is totally absent for the present series. Transition temperatures (Table 3) of a series are mentioned against the number of carbon atoms present in n-alkyl chain of left n-alkoxy terminal end group as determined by an optical polarizing microscopy equipped with a heating stage. Similar or related points were linked to draw smooth curves, Cr-N and N-I, to show the phase behaviors of series as shown in a phase diagram (Figure 1).

Table 3. Transition temperatures of homologous series: α -4-(4'-n-alkoxybenzoyloxy)benzoyl- β -4'-hexadecyloxyphenyl ethylenes.

Compound No.	n-Alkyl chain, $\text{C}_n\text{H}_{2n+1}$	Transition temperatures ($^\circ\text{C}$)		
		Smectic	Nematic	Isotropic
1	C_1	—	—	121.0
2	C_2	—	—	118.0
3	C_3	—	—	124.0
4	C_4	—	—	126.0
5	C_5	—	—	112.0
6	C_6	—	94.0	110.0
7	C_7	—	—	109.0
8	C_8	—	101.0	110.0
9	C_{10}	—	89.0	115.0
10	C_{12}	—	90.0	114.0
11	C_{14}	—	95.0	108.0
12	C_{16}	—	105.0	116.0
13	C_{18}	—	102.0	118.0

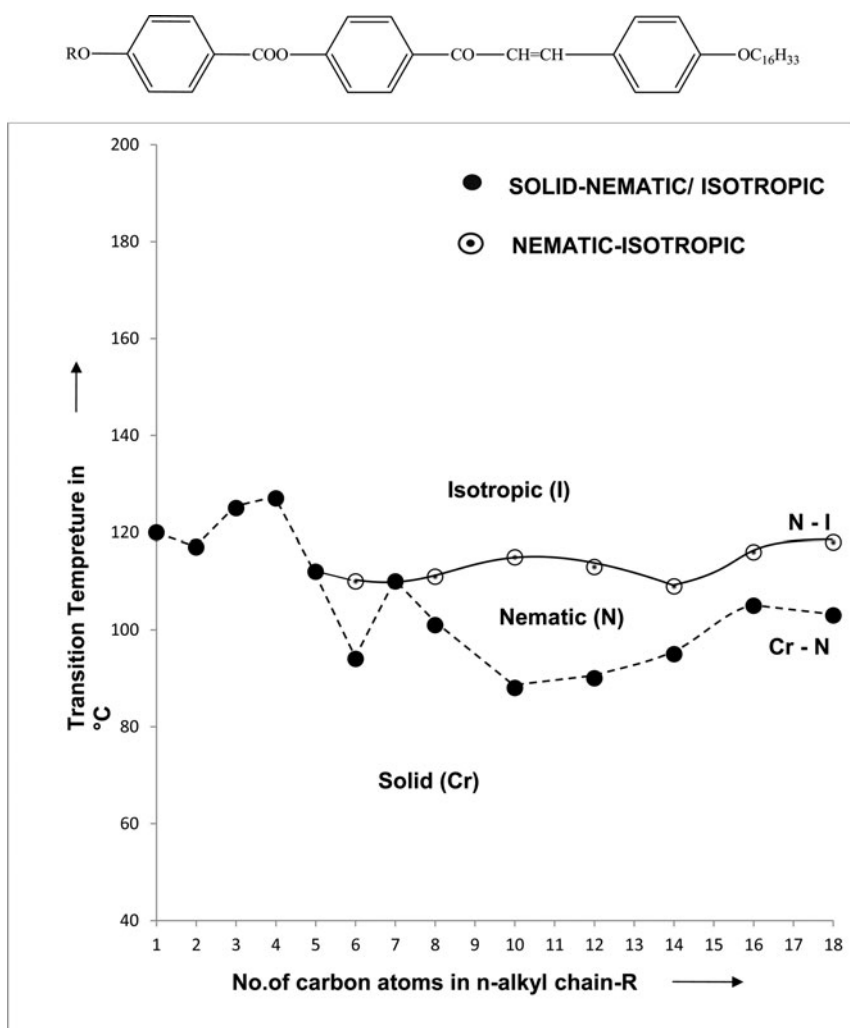


Figure 1. Phase diagram of series 1.

The Cr-N transition curve follows zigzag path of rising and falling with overall descending tendency as series is ascended and behaved in normal manner. N-I transition curves rise by 5°C from C₆ homologue to C₁₀ homologue and then descended to C₁₄ homologue but rises by negligible magnitude for C₁₆ and C₁₈ homologues. Thus, it behaves in a normal manner with negligible deviation for last two higher homologues. Odd-even effect is absent for N-I transition curve. Mesogenic properties from homologue to homologue vary in the present novel series. Textures of nematic mesophase are threaded or Schlieren. Analytical and spectral data confirmed the molecular structures of homologues. Thermal stability for nematic is 113.14°C, whose nematogenic mesophase length ranges from minimum to maximum from 10 to 26°C. Thus, the present homologous series is nematogenic without exhibition of smectic character and lower middle-ordered melting-type.

Lowering of transition temperature of chalconyl ester homologues as compared to corresponding dimeric n-alkoxy acids is attributed to the breaking of hydrogen bonding between two molecules of aromatic acids by esterification process. The exhibition of nematic phase

is attributed to the misalignment of molecules of an angle less than 90° under the externally exposed thermal vibrations of suitable magnitudes that match with the internal energy stored in a molecule (ΔH) as related to the suitable magnitudes of anisotropic forces of intermolecular end-to-end attractions, as a consequence of molecular rigidity and flexibility, which favorably arranges molecules to float on the surface in statistically parallel orientational order to maintain molecular two-dimensional (2D) array. Thus, nematic mesophase appears on the top of microscopic observation. The molecules of homologues maintain characteristic nematic mesophase appearance during N-I transition temperature from C_6 to C_{18} homologues excluding C_7 homologue. However, on continued heating nematogenic homologues from and beyond isotropic temperature (N-I), the molecules are randomly oriented in all possible directions with a high order of disorder in unexpected manner or with high entropy (ΔS). The randomly oriented molecules on cooling from and below isotropic temperature carefully, the nematic mesophase reappears reversibly exactly from and below isotropic temperature until solidification temperature for all present enantiotropic homologues.

The absence of nematic phase or mesophase in C_7 homologue clearly indicates that N-I transition curve passes through Cr-I transition curve, which supports and suggests the non-mesogenic tendency of heptyloxy (C_7) homologue beyond commencement of nematogenic mesophase formation by hexyloxy (C_6) homologue. Non-mesomorphicity of C_5 to C_1 prior to the commencement of nematogenic mesophase formation from C_6 homologue is very well understandable, but absence of nematic phase beyond C_6 requires above explanation. The non-mesomorphic behaviors of C_1 to C_5 and C_7 are attributed to the unsuitable magnitudes of anisotropic forces of intermolecular end-to-end and lateral cohesive forces as a consequence of unfavorable molecular rigidity and flexibility due to their low dipole-dipole interactions and low magnitudes of dispersion forces by interactions between instantaneous dipoles produced by the spontaneous oscillation of electron clouds of molecule, including high crystallizing tendency on cooling. The crystal lattices of non-mesomorphic homologues are breaking abruptly and transform sharply into isotropic liquid without passing through LC state on careful heating. Absence of smectic property is attributed to the absence of lamellar packing of molecules in the crystal lattices of rigid crystals, which hinders the sliding layered molecular arrangements in floating condition under the influence of exposed thermal vibrations. The absence of odd-even effect in N-I transition curves of a phase diagram is due to the absence of nematic phase in C_1 , C_3 , C_5 , and C_7 homologues. Thus, a single N-I transition curve for C_6 , C_8 , C_{10} , C_{12} , C_{14} , C_{16} , and C_{18} homologues appears for phase behaviors of series. The changing trend in thermometric data is attributed to the sequential addition of methylene unit or units in n-alkyl chain bonded to first phenyl ring through oxygen atoms. Added methylene units increase molecular length, permanent dipole-moment across the long molecular axis, dispersion forces, molecular polarity and polarizability, rigidity and flexibility, ΔH value, etc., keeping rest of the molecular part, including tail group $-OC_{16}H_{33}$ intact or unchanged throughout the novel series (C_1 to C_{18}). Thus, variations in intermolecular adhering forces of suitable magnitudes induces and stabilizes nematic mesophase formation from C_6 homologue to C_{18} homologue excluding C_7 homologue. Thus, variations in mesomorphic/LC in properties are attributed to the variation in molecular structure of varying homologues. The present homologous series is nematogenic without exhibition of smectic property, and is of middle-ordered melting-type whose mesophase length ranges from 10 to 26°C . The mesomorphic properties of the present novel series 1 are compared with other structurally known homologous series X [28] and Y [29] as shown in Figure 2.

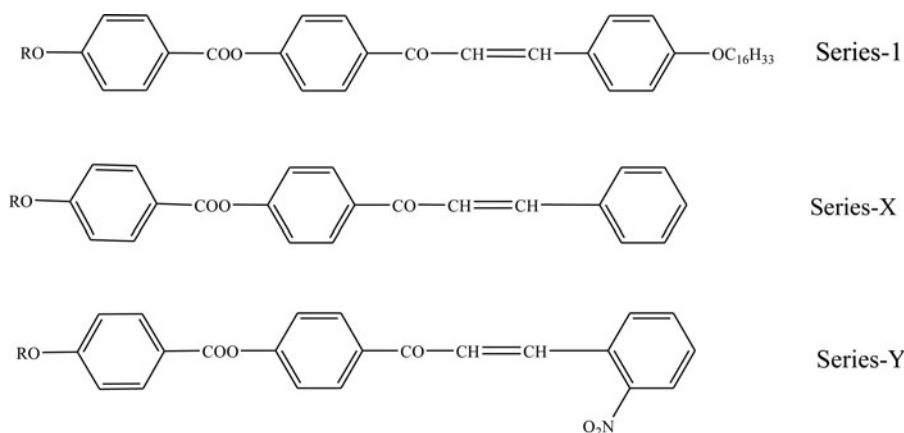


Figure 2. Structurally similar analogous series.

Homologous series 1 of the present investigation and the series X and Y chosen for comparison are identical with respect to three phenyl rings, two central bridges $-\text{COO}-$ and $-\text{CO}-\text{CH}=\text{CH}-$, and the left n -alkoxy terminal end group for the same homologue from series to series. However, series 1, X, and Y differ with respect to tail terminal/lateral end groups $-\text{OC}_{16}\text{H}_{33}$, $-\text{H}$, and $-\text{NO}_2$ respectively. Therefore, they differ with respect to combined effect of molecular rigidity and flexibility as emerged from individual molecular structure for the same homologue from series to series and from homologue to homologue in the same series because the suitable magnitudes of anisotropic forces of intermolecular cohesive forces and closeness vary from homologue to homologue and series to series which undergo variations due to changing permanent dipolemoment across the long molecular axis, dipole–dipole and electronic interactions, dispersion forces, etc. Thus, the variations in LC properties and degree of liquid crystallinity for the same homologue from series to series will depend upon very minute differing features of the molecular structures of individual series and individual homologue of the same series.

Table 4 presents some LC properties of series 1, X, and Y for comparative study. It is clear from Table 4 that homologous series 1 of the present investigation and series X are only nematogenic, whereas Y is nematogenic in addition to smectogenic.

Smectogenic mesophase stabilization is missing for series 1 and X, whereas smectogenic mesophase stabilization is realizable for series Y.

Table 4. Average thermal stability (in $^{\circ}\text{C}$).

Series→	1($-\text{OC}_{16}\text{H}_{33}$)	X($-\text{H}$)	Y(ortho $-\text{NO}_2$)
Smectic–isotropic or smectic–nematic Commencement of smectic phase	—	—	138.0 (C_3-C_{14}) C_3
Nematic–isotropic Commencement of nematic phase	113.14 (C_6-C_{18}) C_6	164.5 (C_6-C_{16}) C_6	163.8 (C_3-C_{16}) C_3
Total mesophase length range ($\text{Sm}+\text{N}$) in $^{\circ}\text{C}$ C_1 to C_p	10.0 to 26.0 C_8 C_{10}	07 to 45.0 C_{16} C_{10}	16.0 to 48.0 C_{16} C_5

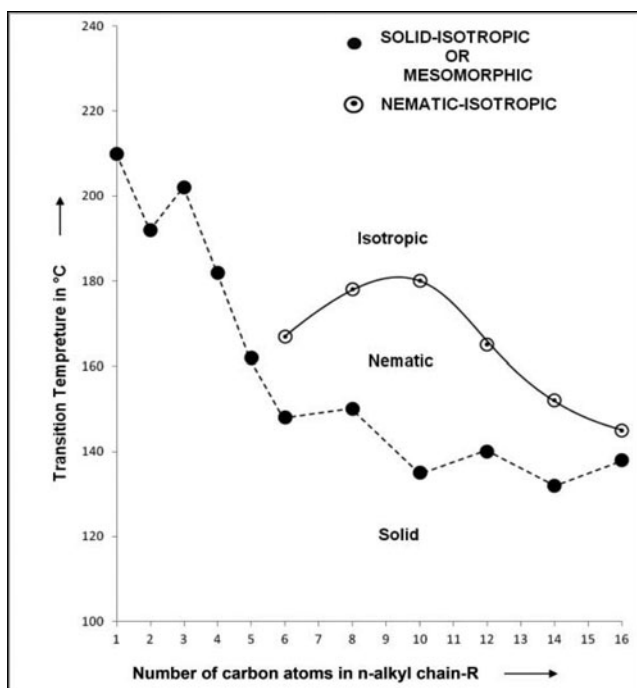


Figure 3. Phase diagram of series X.

Nematic thermal stability of the present series 1 has the lowest value of 113.14 among the series under comparison. The nematic thermal stability of series X and Y is higher than series 1 and is almost equivalent (164.5 and 163.8) to each other.

Smectic and nematic mesophase commence from C_3 homologue for series Y, but only nematic mesophase commences from C_6 homologue of series 1 and X without exhibition of smectic phase.

Mesophase length range is in the increasing order from series 1 to series Y to series X.

Phase diagrams of series X and Y are attached herewith for comparison in [Figures 3 and 4](#).

Lack of smectogenic character by the present series 1 and X is attributed to the absence of lamellar packing of molecules in their crystal lattices due to unsuitable magnitudes of anisotropic forces of intermolecular forces of cohesion to resist exposed thermal vibrations to maintain pre-unoccupied layered structure in rigid crystal. Consequently, absence of layered structure cannot produce sliding layered molecular arrangement to persist and form smectic phase. Thus, inadequate magnitudes of lateral intermolecular attractions fail to exhibit smectogenic character. However, end-to-end attractions occurred by $-OC_{16}H_{33}$ or $-H$ (or unsubstituted phenyl ring) tails as well as left n-alkoxy terminal end group for the same series or series to series, including suitable magnitudes of intermolecular closeness facilitating the formation or environmental situation, which arranges molecules of series 1 and X to float with statistically parallel orientational order only to induce nematogenic character from C_6 homologue.

The exhibition of nematic mesophase in addition to smectic phase in case of series Y is attributed to the ortho-substituted $-NO_2$ lateral group, which increases molecular polarizability. Although broadening or widening of molecule reduces end-to-end attractions, the magnitudes of intermolecular attractions through polarizability increase to such an extent that

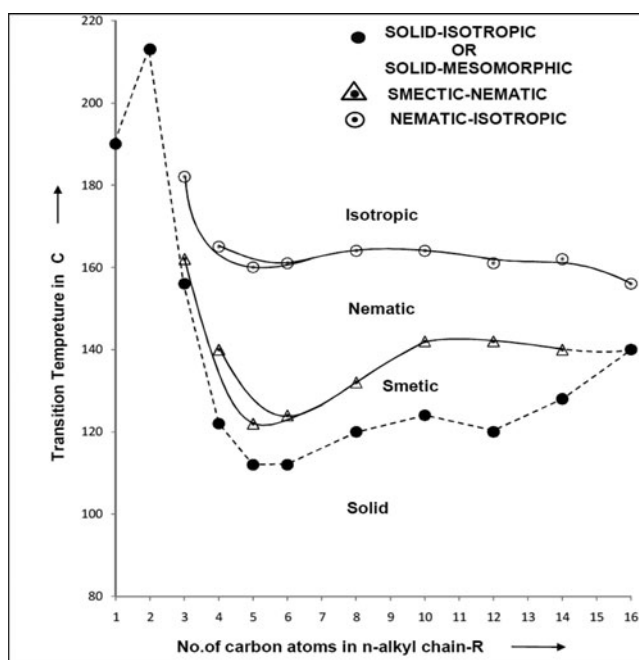


Figure 4. Phase diagram of series Y.

the environmental situation favors sliding layered molecular arrangement at Cr-Sm transition temperature and then statistically parallel orientational order of molecules in floating condition between Sm-N and N-I transition temperatures. Thus, the less polarizable series 1 and X are the missing smectogenic character, and the more polarizable series Y due to lateral substitution facilitated occurrence and exhibition of smectic property in addition to nematic property. The phase stabilization energy is related to the energy stored in a molecule at constant pressure (ΔH) and the suitable magnitudes of anisotropic forces of intermolecular attractions and closeness which induce LC state between two temperatures, depending upon the thermal resistivity of individual homologue till the frequency of externally exposed thermal vibrations of internal cohesive energy matches. Thus, mesophase stabilization (average) is originated and facilitated from molecular structure of individual substance, which varies from substance to substance and series to series. Increasing order of total mesophase length range from series 1 to Y to X is attributed to the combined positive effect of molecular rigidity and/or flexibility responsible to commence and continue the facilitation of formation of LC state depending upon molecular structure. Thus, differing features of structurally similar homologous series for the same homologue from series to series and from homologue to homologue of the same series exhibit different degrees of mesomorphic behaviors and mesomorphism. Hence, the present novel series 1, although possesses the longest para-substituted tail group $-\text{OC}_{16}\text{H}_{33}$, has a limited impact on LC properties and the degree of mesomorphism because it induces less ordered nematogenic mesophase of low degree of mesophase length range and the late commencement (from C_6) of LC (nematic) phase.

Conclusions

The present novel series of chalconyl ester derivatives is nematogenic without exhibition of smectic property, whose degree of mesomorphism is low and is of lower middle-ordered melting-type.

A longer n-alkyl chain is bonded to phenyl ring through the oxygen atom whose flexibility is less effective to induce mesomorphism in a substance.

Group efficiency order derived based on (i) thermal stability, (ii) early commencement of mesophase, and (iii) total mesophase length range for smectic and nematic are as under:

(i) Smectic: ortho $-\text{NO}_2 > -\text{H} = -\text{OC}_{16}\text{H}_{33}$

Nematic: $-\text{H} \approx \text{ortho } -\text{NO}_2 > -\text{OC}_{16}\text{H}_{33}$ (164.5) (163.8)

(ii) Smectic: ortho $-\text{NO}_2 > -\text{H} = -\text{OC}_{16}\text{H}_{33}$

Nematic: ortho $-\text{NO}_2 > -\text{H} = -\text{OC}_{16}\text{H}_{33}$

(iii) (Smectic \pm Nematic): $-\text{H} > \text{ortho } -\text{NO}_2 > -\text{OC}_{16}\text{H}_{33}$

Molecular rigidity and flexibility depends upon molecular structure.

Mesomorphism is very sensitive and susceptible to molecular structure.

The present investigation may be useful for the study of binary systems for thermotropic LC devices.

Chalconyl derivatives being biologically active in lyotropic condition may be useful for pharmaceutical preparations.

Acknowledgments

Authors acknowledge thanks to Dr. R.R. Shah, principal of K.K. Shah Jarodwala Maninagar Science College, Ahmedabad. Authors are also thankful to Dr. A.V. Doshi, Ex-principal of M.V.M. Science College, Rajkot, for his constant support, inspirations, and help, as and when needed during the course of present investigation. Authors thank to NFDD Centre for the analytical and spectral services.

References

- [1] Reinitzer, F. (1888). *Monatsh*, 9, 421.
- [2] Narmura, S. (2001). *Displays*, 22(1), 1.
- [3] Kim, W. S., Elston, S. J., & Ranyes, F. P. (2008). *Displays*, 29, 458–463.
- [4] Tadwee, I., Sahanashahi, Ramteke, V., & Syed, I. (2012). *IJPRAS*, 1(2), 06–11 (ISSN 2277–2236).
- [5] Hertz, E., Lavoreh, B., & Faucher, O. (2011). *Nature Photon*, 5, 78–79.
- [6] Calliste, C. A., Bail, J. C. Le., Trouilar, P., Pouget, C., Chulia, A. J., & Duroux, L. J. (2001). *Anticancer Res.*, 21, 3949–3956.
- [7] Rajesh, G., Mansi, K., Srikant, K., Babasaheb, B., Nagesh, D., Kavita, S., & Ajay, C. (2008). *Chem. Pharm. Bull.*, 56, 897–901.
- [8] Gray, G. W. & Winsor, P. A. (1964). *Liquid Crystals and Plastic Crystals*, vol. 1, Ellis Horwood, Chichester, pp. 103–152.
- [9] Jain, Upendra K., & Irun, S. (2014). *Trop. J. Pharm. Res.*, 139(1), 73–80.
- [10] Gaikwad, P. P., & Desai, M. T. (2013). *Int. J. Pharm. Res. Rev.*, 2(12), 40–52.
- [11] Imrie, C. T. (1999). *Liq. Cryst. Dimers Struct. Bond*, 95, 149–192.
- [12] Gray, G. W. (1974). In *Liquid Crystal and Plastic Crystal*, edited by G. W. Gray and P. A. Winsor, (Horwood, Chichester), Chap. 4, pp. 103–152.
- [13] Gray, G. W. (1962). *Molecular Structures and Properties of Liquid Crystals*, Academic Press: London.
- [14] Demus, D. (1988). *Mol. Cryst. Liq. Cryst.*, 165, 45–84.
- [15] Demus, D. (1989). *Mol. Struct. Liq. Cryst.*, 5, 75–100.
- [16] (i) Suthar, D. M., & Doshi, A. V. (2013). *Mol. Cryst. Liq. Cryst.*, 575 76–83. (ii) Chauhan, H. N., & Doshi, A. V. (2013). *Mol. Cryst. Liq. Cryst.* 570, 92–100. (iii) Chaudhari, R. P., Chauhan, M. L. & Doshi, A. V. (2013). 575, 88–95. (iv) Bhoya, U. C., Vyas, N. N., & Doshi, A. V. (2012). *Mol. Cryst. Liq. Cryst.*, 552, 104–110.
- [17] Marathe, R. B., & Doshi, A. V. (2016). 624(1), 144.
- [18] Suthar, D. M., Doshi, A. A., & Doshi, A. V. (2013). *Mol. Cryst. Liq. Cryst.* 582, 79–87.
- [19] Henderson, P. A., Niemeyer, O., & Imrine, C. T. (2001). *Liq. Cryst.* 28, 463–472.

- [20] Patel, B. H., & Doshi, A. V. (2015). *Mol. Cryst. Liq. Cryst.*, 605, 23–31.
- [21] Colling, P. J., & Hird, M. (1998). *Introduction to Liquid Crystal Chemistry and Physics*, Taylor and Francis: London.
- [22] Marcos, M., Omenant, A., Serrano, J. L., & Ezcurra, A. (1992). *Adv. Matter*, 4, 285
- [23] Hird, M., Toyne, K. J., & Grey, G. W. (1993). *Liq. Cryst.*, 14, 741.
- [24] Patel, B. H., & Doshi, A. V. (2015). *Mol. Cryst. Liq. Cryst.*, 605, 42–51.
- [25] Dave, J. S., & Vora, R. A. (1970). In: *Liquid Crystals and Ordered Fluids*, J. F. Johnson & R. S. Porter (Eds.), Plenum Press: New York, NY, p. 477.
- [26] Suthar, D. M., Doshi, A. A., & Doshi, A. V. (2013). *Mol. Cryst. Liq. Cryst.*, 527, 51–58.
- [27] Bhoya, U. C., Vyas, N. N., & Doshi, A. V. (2012). *Mol. Cryst. Liq. Cryst.*, 552, 104–110.
- [28] Chauhan, H. N., Patel, V. R., & Doshi, A. V. (2013). *Mol. Cryst. Liq. Cryst.*, 574, 67–74.
- [29] Chauhan, H. N., & Doshi, A. V. (2013). *Mol. Cryst. Liq. Cryst.*, 570, 92–100.